MOLECULAR PLANT PATHOLOGY (2009) **10**(2), 237–248 DOI: 10.1111/J.1364-3703.2008.00526.X

Functional characterization of transcripts expressed in early-stage *Meloidogyne javanica*-induced giant cells isolated by laser microdissection

JOHN FOSU-NYARKO, MICHAEL G. K. JONES AND ZHAOHUI WANG*

Plant Biotechnology Research Group, Western Australian State Agricultural Biotechnology Centre (SABC), School of Biological Sciences and Biotechnology, Murdoch University, Perth, WA6150, Australia

SUMMARY

The root-knot nematode *Meloidogyne javanica* induces giant cells and feeds from them during its development and reproduction. To study the cellular processes underlying the formation of giant cells, laser microdissection was used to isolate the contents of early-stage giant cells 4 and 7 days post-infection (dpi) from tomato, and cDNA libraries from both stages were generated with 87 [250 expressed sequence tag (EST) clones] and 54 (309 EST clones) individual transcripts identified, respectively. These transcripts have roles in metabolism, stress response, protein synthesis, cell division and morphogenesis, transport, signal transduction, protein modification and fate, and regulation of cellular processes. The expression of 25 selected transcripts was studied further by real-time quantitative reverse transcriptase-polymerase chain reaction. Among them, 13 showed continuous up-regulation in giant cells from 4 to 7 dpi. The expression of two transcripts was higher than in controls at 4 dpi and remained at the same level at 7 dpi; a further five transcripts were highly expressed only at 7 dpi. The Phi-1 protein gene, a cell cycle-related homologue in tobacco, was expressed 8.5 times more strongly in giant cells than in control cells at 4 dpi, but was reduced to 6.7 times at 7 dpi. Using *in situ* hybridization, the expression of the *Phi-1* gene was preferentially localized in the cytoplasm of giant cells at 4 dpi, together with a pectinesterase U1 precursor gene. The identification of highly expressed transcripts in developing giant cells adds to the knowledge of the plant genes responsive to nematode infection, and may provide candidate genes for nematode control strategies.

INTRODUCTION

Sedentary endoparasitic nematodes are the most economically important group of plant parasitic nematodes. They are obligate biotrophs and have intimate relationships with their hosts, where they can control the development of host cells after infection (Jones, 1981). Root-knot nematodes (*Meloidogyne* spp.) establish feeding sites from provascular cells of the host root, and these act as the sole source of nutrition for the development and reproduction of the nematode. Several distinct processes occur during the establishment of feeding sites. J2 juveniles (J2s) invade roots behind the root tip, and then migrate between cells to reach the developing vascular cylinder. The J2s introduce secretions from their oesophageal gland cells into a group of selected provascular cells which re-enter the cell cycle (Davis *et al.*, 2000; Jones and Payne, 1978). These cells undergo repeated nuclear divisions without cytokinesis to form larger multinucleate cells, known as giant cells (Jones, 1981). Cortical cells around the developing giant cells also divide rapidly and expand to form a gall.

The expansion of giant cells and cytoskeleton rearrangements end at 10–14 days post-infection (dpi) (de Almeida Engler *et al.*, 2004; Jones, 1981). They become filled with dense cytoplasm and contain many organelles (Jones, 1981). Giant cells also have a high osmotic potential. From about 3 dpi, transfer cell-like wall ingrowths form next to vascular tissues; these ingrowths become very extensive and increase the surface area of the cell membrane by up to 10-fold to facilitate the uptake of nutrients to the developing nematode (Jones and Dropkin, 1976). These physiological and biochemical changes are accompanied by alterations in gene expression, not only in the giant cells, but also in neighbouring cells.

In studies on the responses of host plants to nematode infection, a number of differentially expressed genes have been identified in infected root tissues relative to control roots (Bird and Wilson, 1994; Fuller *et al.*, 2007; Jammes *et al.*, 2005; Wang *et al.*, 2003). Other approaches have involved promoter trapping and transcriptional studies with β-glucuronidase (GUS) (Favery *et al.*, 1998, 2004; Goddijn *et al.*, 1993), and the localization of expression of nematode responsive genes by *in situ* hybridization (Escobar *et al.*, 2003; Lohar *et al.*, 2004). However, as giant cells make up only a small fraction of the root cells, the analysis of gene expression at the single-cell level is required to study these highly specialized nematode feeding cells (Ramsay *et al.*, 2004).

**Correspondence*: Tel.: 61 8 9360 2920; Fax: 61 8 9360 6303; E-mail: zwang@murdoch.edu.au

Until recently, the isolation of cytoplasmic contents from nematode feeding cells was limited to manual dissection and microaspiration (Bird and Wilson, 1994; Jammes *et al.*, 2005; Juergensen *et al.*, 2003; Wang *et al.*, 2003). The feeding cell-enriched tissues or giant cell contents obtained from such techniques have been subjected to molecular analysis, including the use of microarrays to study the genome-wide expression profiles of *Arabidopsis* infected with root-knot nematodes (Jammes *et al.*, 2005; Wang *et al.*, 2003). However, there are limitations to these methods, in that they cannot be applied effectively to study the early stages of development of giant cells.

Laser microdissection (LM) provides a solution to the isolation of the cytoplasmic contents from specific plant cells, including early-stage nematode feeding cells (Day *et al.*, 2005; Ramsay *et al.*, 2006). Klink *et al.* (2005) constructed a syncytium-specific cDNA library from mRNA obtained by LM of soybean roots infected with the soybean cyst nematode *Heterodera glycines* at 8 dpi. LM has also been coupled with the microarray technique to provide a comprehensive gene expression profile of developing syncytia in soybean roots induced by *H. glycines* (Ithal *et al.*, 2007a). It is well established that there are fundamental differences between the development of syncytia and giant cells (Gheysen and Fenoll, 2002; Jones, 1981). The identification of changes in gene expression in giant cells using LM will advance the current knowledge of the processes of their induction, development and maintenance, and add to our understanding of the differences in development between giant cells and syncytia.

In this study, we have constructed two cDNA libraries using LM to isolate total RNA from early-stage giant cells, 4 and 7 days after nematode infection. The transcripts known to be involved in a range of key cellular and biological processes, including the genes involved in cell division, metabolism (carbohydrate, lipid, energy, and nucleotide and amino acid) and cellular transport, were identified. The temporal and spatial analysis of gene expression of some of the transcripts identified was also performed. The differences in the cellular processes involved in the formation and development of giant cells and syncytia are discussed.

RESULTS

RNA from developing giant cell contents obtained by LM

A PALM Robot-Combi LM system was used to isolate the cytoplasmic contents of early-stage giant cells induced by *Meloidogyne javanica* from the roots of *in vitro*-cultured tomato. Root galls were fixed, embedded in paraffin wax, sectioned and de-waxed. Giant cell initials were clearly visible in treated sections and the morphology was adequately preserved. This allowed the identification and isolation of the contents of the developing giant cells (Fig. 1). As a control for the quantification of gene expression, cells adjacent to the vascular cylinder were similarly isolated from *in vitro*-cultured tomato roots at the same age as the infected roots, but without nematode infection. For cDNA

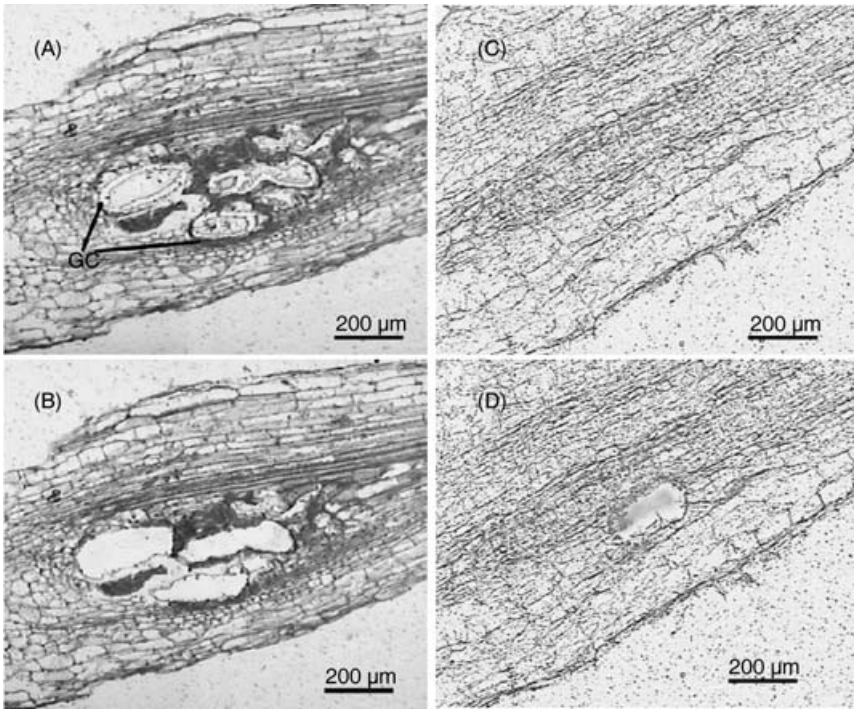

Fig. 1 Laser microdissection (LM) of giant cells induced by the root-knot nematode *Meloidogyne javanica* on roots of tomato. (A, B) Longitudinal sections through the root showing early-stage giant cells before dissection (A) and with cell contents removed after LM (B). (C, D) Longitudinal sections through the root of a control plant (C) showing region of cells close to the vasculature (D) captured as control cells to calibrate gene expression of giant cell transcripts. GC, giant cells.

library construction, 100 ng of total RNA obtained from laser microdissected cells was subjected to two rounds of linear amplification using a T7 RNA-based polymerase system to give up to 100 μg of amplified RNA (aRNA), which was also used for real-time quantitative reverse transcriptase-polymerase chain reaction (RT-PCR) analysis.

Transcript profile of giant cells at 4 dpi

The 4-dpi giant cell-specific cDNA library was constructed from cDNA synthesized from aRNA primed with Oligo-dT and random hexamers. The expressed sequence tag (EST) clones were initially screened by PCR and restriction enzyme digestion analysis, and those selected for sequencing had an insert of at least 70 bp. The analysis of 250 EST clones generated 87 individual sequences (Table 1). The size of the cDNA inserts ranged from 76 to 648 bp. All the sequences have been submitted to the National Center for Biotechnology Information (NCBI) GenBank with accession numbers ES790116–ES790201. Most of the transcripts were identified stringently as tomato sequences when compared with the tomato gene index database from *The Gene Index Project* using the 'blast' search tool, most of which are known to express in tissues other than the root system. Some other transcripts were identified as homologues of genes sequenced from other plant species from the NCBI database, including *Solanum tuberosum*, *Arabidopsis thaliana*, *Nicotiana tabacum* and *Nicotiana benthamiana*, and also monocots, such as *Oryza* spp., *Triticum aestivum* and *Zea mays*. Eight of the transcripts did not match any known gene or protein sequence. Instead, they were identified as cDNA sequences from tomato (ES790139, ES790144, ES790156 and ES790178), *S. tuberosum* (ES790121, ES790125, ES790142 and ES790167) or *Nicotiana* spp. (ES790125). The transcript ES790177 had no similar match on any database.

Transcript profile of giant cells at 7 dpi

From aRNA obtained from giant cells at 7 dpi, 54 individual transcripts with sizes ranging from 81 to 610 bp were obtained from the sequencing of 309 cDNA clones (Table 2). These have accession numbers ES790202–ES790255 in the NCBI GenBank. From the blast search results, 42 of the transcripts matched characterized genes of tomato, *Medicago truncatula* and *A. thaliana*. The sequences of seven transcripts (ES790212, ES790224, ES790225, ES790232, ES790248, ES790249 and ES790255) did not match any characterized gene in the databases, although mRNA and/or cDNA sequences with significant matches have been identified from other plant species. For instance, clones of identical sequences to ES790212 exist in databases for cDNA from trichomes of *N. benthamiana* (GenBank Accession No. ES887635.1) and *Humulus lupulus* (L. cv. Phoenix) (GenBank Accession No. ES658159.1).

Functional characterization of giant cell transcripts

To understand the biological processes that govern the establishment of giant cells, the transcripts obtained from the giant cell-specific libraries constructed at 4 and 7 dpi were classified into functional groups using UNIProt and the *Kyoto Encyclopaedia of Genes and Genomes*, and relevant descriptions and motifs of homologues in databases. The classification was performed on the basis of the cellular processes that are likely to be involved in the induction and development of giant cells, including several signal transduction pathways, cell division and expansion, transport, DNA replication and protein synthesis associated with high metabolic activities (Tables 1 and 2).

Several genes that are putative components of signal transduction pathways were identified. These included LescPth2 (a serine/threonine protein kinase), which is a component of the pathway involved in the M phase of the cell cycle, a putative serine/arginine (SR) protein kinase, a G-protein-coupled receptor-like protein and a homologue of the *A. thaliana* putative receptor protein kinase PERK1. The presence and initial movement of J2s between cells may activate defence and stress transduction pathways in the host root. This is suggested by the identification of the heat shock cognate 70-kDa protein, cytosolic copper, zinc and manganese superoxide dismutase, ethylene responsive factors, early light-inducible protein, pathogenesis-related proteins TSI-1 and the *S. tuberosum* ssp. *andigena* ry-1 resistance gene, all of which are known to be involved in defence and cellular responses to biotic and abiotic stresses.

Five individual genes involved in cell division and cell wall morphogenesis were identified in the 4-dpi library. These included a tomato homologue of the tobacco Phi-1 protein, two pectin methylesterases and a pectinesterase U1 precursor. An F-box-containing protein known to regulate diverse cellular processes, including cell cycle transition, transcriptional regulation and signal transduction, was also identified in the 4-dpi library. The process of cell re-differentiation to produce giant cells will employ a rapid DNA processing machinery, evidenced in the identification of several DNA-binding proteins, including transcription factors [e.g. transcription initiation factor IIB (TFIIB), Scarecrow-like 8 transcription factor, Zinc finger, AP2/ERF] and other structural and functional components involved in DNA synthesis, such as histones (e.g. Histone 1, 2B-like and 4), ribonucleoprotein complexes (e.g. ribonucleoprotein complex subunit 2-like protein) and RNA polymerases.

Many genes directly involved in protein synthesis, modification and degradation were identified from both libraries. These included 15 ribosomal proteins, two RNA-binding proteins (e.g. RNA-binding protein RZ-1) and a DNA-directed RNA polymerase II polypeptide K. The ubiquitin–proteasome pathway, which plays a key role in many cellular processes, including cell cycle control, hormonal signal transduction, flower development and circadian

Table 1 Transcripts identified in the 4 days post-infection (dpi) cDNA library generated from laser microdissected giant cells induced in tomato roots by *Meloidogyne javanica*.

Clone	GenBank Accession No.	Highest homology search results	Functional category	BLAST score
4LCMGC001	ES790116	Hypothetical protein {*Arabidopsis thaliana*}	Unclassified protein	2.10E-29
4LCMGC002	ES790117	Hydroxymethylglutaryl coenzyme A synthase	Metabolism	7.70E-50
4LCMGC003	ES790118	Pyruvate dehydrogenase E1 α subunit	Metabolism	2.30E-34
4LCMGC004	ES790119	Fibre protein Fb15	Unknown function	1.80E-116
4LCMGC005	ES790120	60S ribosomal protein L7A-like	Cellular component, protein synthesis	1.60E-117
4LCMGC006	ES790121	cDNA sequence {*Solanum tuberosum*}	Unknown function	5.00E-94
4LCMGC007	ES790122	Unknown protein {*A. thaliana*}	Unclassified protein	7.00E-61
4LCMGC008	ES790123	Clathrin binding {*A. thaliana*}	Intercellular transport	2.60E-49
4LCMGC009	ES790124	DnaJ-like protein	DNA processing	1.90E-39
4LCMGC010	ES790125	cDNA sequence from *Solanum tuberosum, Nicotiana* spp.	Unknown function	8.00E-11
4LCMGC011	ES790126	Peptidyl-prolyl *cis–trans* isomerase (cyclophilin)	Protein modification	4.00E-37
4LCMGC012	ES790127	Lipid transfer protein, PVR3-like protein	Transport	4.70E-41
4LCMGC013	ES790128	Expressed protein {*A. thaliana*}	Unclassified protein	2.50E-12
4LCMGC014	ES790129	*S*-Adenosylmethionine decarboxylase	Metabolism, amino acid	1.00E-15
4LCMGC015	ES790256	Protein translation factor SUI1 homologue (GOS2 protein)	Protein synthesis	3.00E-37
4LCMGC016	ES790130	40S ribosomal protein S8	Cellular component, protein synthesis	6.60E-24
4LCMGC017	ES790131	28-kDa small subunit ribosomal protein	Cellular component, protein synthesis	5.70E-16
4LCMGC018	ES790132	Transaldolase	Metabolism, carbohydrate	2.00E-56
4LCMGC019	ES790133	Unknown protein {*A. thaliana*}	Unclassified protein	1.50E-67
4LCMGC020	ES790134	Calmodulin-like protein	Regulation of cellular activities	1.4E-35
4LCMGC021	ES790135	Cyclopropane fatty acid synthase	Metabolism, lipid	1.30E-22
4LCMGC022	ES790136	Histone H1	DNA processing	1.20E-16
4LCMGC023	ES790137	F-box-containing protein	Cell cycle regulation, signal transduction	2.60E-82
4LCMGC024	ES790138	Hypothetical protein {*A. thaliana*}	Unclassified protein	5.30E-40
4LCMGC025	ES790139	cDNA sequence {*Lycopersicon esculentum*}	Unknown function	4.80E-58
4LCMGC026	ES790140	Unknown protein {*A. thaliana*}	Unclassified protein	3.40E-59
4LCMGC027	ES790141	Early light-inducible protein	Thylakoid biogenesis and rescue	2.00E-108
4LCMGC028	ES790142	cDNA sequence {*S. tuberosum*}	Unknown function	4E-86
4LCMGC029	ES790143	Glyceraldehyde 3-phosphate dehydrogenase	Metabolism, energy	5.70E-44
4LCMGC030	ES790144	cDNA sequence {*L. esculentum*}	Unknown function	2.7E-56
4LCMGC031	ES790145	Cytochrome P450 monooxygenase CYP72B	Electron transfer	1.50E-90
4LCMGC032	ES790146	Cytosolic Cu,Zn superoxide dismutase (LeSODCC)	Regulation of cellular processes	8.90E-13
4LCMGC033	ES790147	ChaC-like family protein-like	Unclassified protein	2.20E-34
4LCMGC034	ES790148	60S ribosomal protein L30	Cellular component, protein synthesis	1.50E-26
4LCMGC035	ES790149	Ethylene response factor 5	Transcription	3.50E-18
4LCMGC036	ES790150	ELI3 protein	Metabolism, carbohydrate	8.20E-13
4LCMGC037	ES790151	Chaperonin 21 precursor	Protein modification	1.80E-80
4LCMGC038	ES790152	Aspartyl aminopeptidase	Metabolism, amino acid	6.50E-20
4LCMGC039	ES790153	LescPth2, serine/threonine protein kinase Fen	Signal transduction	1.20E-06
4LCMGC040	ES790154	Unknown protein, heavy-metal-associated domain putative	Unknown function	2.80E-37
4LCMGC041	ES790155	Proteasome subunit β type 2-A	Protein modification	2.20E-84
4LCMGC042	ES790156	cDNA sequence {*L. esculentum*}	Unknown function	3.40E-27
4LCMGC043	ES790157	60S ribosomal protein L15	Cellular component, protein synthesis	3.60E-12
4LCMGC044	ES790158	Unknown protein {*A. thaliana*}	Unclassified protein	6.80E-19
4LCMGC045	ES790159	Transcription factor {*A. thaliana*}	Transcription	2.50E-34
4LCMGC046	ES790160	Transaldolase	Metabolism, carbohydrate	2.00E-56
4LCMGC047	ES790161	RING-H2 finger protein RHG1a-like	Transcription	9.70E-20
4LCMGC048	ES790162	NADPH cytochrome P450 reductase CprA {*Aspergillus fumigatus* Af293}	Electron transfer	6.40E-59
4LCMGC049	ES790163	Heat shock protein 70-3	Regulation of cellular activities	1.90E-29
4LCMGC050	ES790164	Putative CPF 0172 family protein {*A. thaliana*}	Unclassified protein	4.00E-73
4LCMGC051	ES790165	Pectinesterase U1 precursor (pectin methylesterase)	Cell division and cellular morphogenesis	3.30E-25

Table 1 *Continued.*

Clone	GenBank Accession No.	Highest homology search results	Functional category	BLAST score
4LCMGC052	ES790166	Calmodulin-binding protein	Regulation of cellular activities	1.20E-49
4LCMGC053	ES790167	cDNA sequence {*S. tuberosum*}	Unknown function	2E-154
4LCMGC054	ES790168	2-Oxoglutarate-dependent dioxygenase	Metabolism, energy	6.10E-63
4LCMGC055	ES790169	Cinnamyl alcohol dehydrogenase (CAD)	Metabolism, biosynthesis of secondary metabolites	8.20E-20
4LCMGC056	ES790170	Hypothetical protein {*A. thaliana*}	Unclassified protein	3.70E-73
4LCMGC057	ES790171	Ribosomal protein 117	Cellular component, protein synthesis	9.8E-17
4LCMGC058	ES790172	ADP-ribosylation factor-like protein	Signal transduction	2.50E-24
4LCMGC059	ES790173	Histone H2B	DNA processing	9.40E-42
4LCMGC060	ES790174	Phenylalanine ammonia-lyase	Metabolism, biosynthesis of secondary metabolites	1.70E-36
4LCMGC061	ES790175	Zinc finger transcription factor-like protein	Transcription	4.90E-11
4LCMGC062	ES790176	G-protein-coupled receptor-like protein	Signal transduction	8.60E-23
4LCMGC063	ES790177	No match to a known sequence		
4LCMGC064	ES790178	cDNA sequence {*L. esculentum*}	Unknown function	2.90E-73
4LCMGC065	ES790179	Clathrin-binding protein-like {*A. thaliana*}	Protein modification	1.40E-97
4LCMGC066	ES790180	RNA polymerase II largest subunit (fragment)	Transcription	2.90E-09
4LCMGC067	ES790181	Zinc finger protein	Transcription	2.20E-32
4LCMGC068	ES790182	Putative receptor protein kinase PERK1 {*A. thaliana*}	Signal transduction	7.30E-79
4LCMGC069	ES790183	RNA-binding protein putative	Protein synthesis	3.40E-19
4LCMGC070	ES790184	Putative uncharacterized protein {*A. thaliana*}	Unclassified protein	7.50E-41
4LCMGC071	ES790185	Pectin methylesterase (PMEU1)	Cell division and cellular morphogenesis	6.00E-66
4LCMGC072	ES790186	AP2/ERF-domain protein	Transcription	5.80E-21
4LCMGC073	ES790187	Sugar-phosphate isomerase-like protein	Metabolism, carbohydrate	4.10E-51
4LCMGC074	ES790188	Ubiquitin-conjugating enzyme UBC2	Protein modification	7.90E-54
4LCMGC075	ES790189	Phi-1 protein (*Nicotiana tabacum*}	Cell division and cellular morphogenesis	2.20E-56
4LCMGC076	ES790190	Pectinesterase-like protein	Cell division and cellular morphogenesis	4.40E-21
4LCMGC077	ES790191	Unknown protein {*A. thaliana*}	Unclassified protein	1.50E-29
4LCMGC078	ES790192	Microtubule-associated protein MAP65-1a	Unclassified protein	3.1E-28
4LCMGC079	ES790193	Methionine synthase	Metabolism, amino acid	5.50E-82
4LCMGC080	ES790194	Pathogenesis-related TSI-1 protein	Defence related	4.70E-20
4LCMGC081	ES790195	Arginine decarboxylase	Metabolism, amino acid	4.60E-46
4LCMGC082	ES790196	Resistance gene-like, *S. tuberosum* ssp. *andigena* ry-1 gene	Defence related	1E-25
4LCMGC083	ES790197	Ubiquitin-protein ligase {*A. thaliana*}	Protein modification	2.7E-82
4LCMGC084	ES790198	Transcription initiation factor IIB (TFIIB)	Transcription	4.90E-125
4LCMGC085	ES790199	PIP-type aquaporin	Cellular transport	2.70E-21
4LCMGC086	ES790200	Expressed but uncharacterized protein {*A. thaliana*}	Unclassified protein	5.00E-58
4LCMGC087	ES790201	Probable 60S ribosomal protein L32, mitochondrial precursor	Cellular component, protein synthesis	3.70E-22

rhythm, was well represented in the libraries. Enzymes representing the three main enzymatic reactions governing the ubiquitination of target proteins were present in the libraries: 26S proteasome regulatory particle, ubiquitin-conjugating enzyme UBC2 and ubiquitin-protein ligase, also known to be involved in the maintenance of cell viability during root development in rice. Other genes identified in the libraries, which are involved in protein folding and fate, included cyclophilins, a chaperone precursor and a homologue of the *A. thaliana* Calreticulin 3. Consistent with alterations in metabolic activities in nematode feeding sites, many genes encoding proteins involved in different pathways in energy, carbohydrate and amino acid metabolism were identified from both giant cell-specific libraries. Only one gene, for a cyclopropane fatty acid synthase, was cloned that was directly involved in lipid metabolism.

Genes involved in cellular transport and intercellular communication were also identified, including a PIP-type aquaporin and a non-specific lipid transfer protein, similar to the PVR3 protein and known to be a root-specific protein in beans and pineapple. Clathrin and clathrin-binding proteins, which are part of an oligomeric complex of coat proteins regulating vesicular traffic through the Golgi complex and from the Golgi to the endoplasmic reticulum, were represented in the library. Calcium-binding proteins regulate changes in the concentration of

Table 2 Transcripts identified in the 7 days post-infection (dpi) cDNA library generated from laser microdissected giant cells induced in tomato roots by *Meloidogyne javanica*.

Clone	GenBank Accession No.	Highest homology search results	Functional category	blast score
7LCMGC001	ES790202	Ribosomal protein L27	Cellular component, protein synthesis	7.70E-17
7LCMGC002	ES790203	Putative protein {*Arabidopsis thaliana*}	Unclassified proteins	1.50E-24
7LCMGC003	ES790204	Putative membrane-associated protein {*A. thaliana*}	Unknown function	3.10E-14
7LCMGC004	ES790205	Putative protein {*A. thaliana*}	Unclassified proteins	4.20E-23
7LCMGC006	ES790207	Histone H4 {*Capsicum annuum*}	DNA processing	4.70E-47
7LCMGC007	ES790208	26S proteasome regulatory particle triple-A ATPase subunit 2b	Protein modification	2.50E-26
7LCMGC008	ES790209	Metallothionein-like protein type 2	Detoxification (regulation) of heavy metals in cells c	9.50E-24
7LCMGC009	ES790210	Peptidyl-prolyl *cis–trans* isomerase (cyclophilin)	Protein modification	5.20E-14
7LCMGC010	ES790211	40S ribosomal protein S15-like	Cellular component, protein synthesis	2.20E-42
7LCMGC011	ES790212	cDNA sequence cloned from several plant species	Unknown function	4.00E-47
7LCMGC012	ES790213	Unknown protein {*A. thaliana*}	Unclassified proteins	2.00E-49
7LCMGC013	ES790214	Chloroplast rRNA-operon	Protein synthesis	3.60E-64
7LCMGC014	ES790215	Phenylalanine ammonia-lyase (PAL)	Metabolism, biosynthesis of secondary metabolites	1.80E-43
7LCMGC015	ES790216	Lethal leaf spot 1-like protein	Regulation of cellular processes	2.40E-56
7LCMGC016	ES790217	ATPP2-A15 {*A. thaliana*}	Unknown function	8.40E-38
7LCMGC017	ES790218	Scarecrow-like 8 transcription factor	Transcription	7.60E-08
7LCMGC018	ES790219	Cytochrome oxidase subunit 3	Metabolism, electron transport	6.20E-19
7LCMGC019	ES790220	Probable nucleolar GTP-binding protein 1	Signal transduction	2.10E-19
7LCMGC020	ES790221	Heat shock cognate 70-kDa protein	Regulation of cellular processes	7.70E-53
7LCMGC021	ES790222	Annexin p34	Membrane traffic and signal transduction among others	6.50E-44
7LCMGC022	ES790223	Expressed protein {*A. thaliana*}	Unclassified proteins	1.20E-09
7LCMGC023	ES790224	cDNA sequence cloned from several plant species	Unknown function	1.00E-79
7LCMGC024	ES790225	cDNA sequence {*Lycopersicon esculentum*}	Unknown function	3.00E-92
7LCMGC025	ES790226	60S ribosomal protein L7A-like	Cellular component, protein synthesis	4.00E-43
7LCMGC026	ES790227	CRT3 (Calreticulin 3) {*A. thaliana*}	Protein modification	3.50E-37
7LCMGC027	ES790228	Manganese superoxide dismutase	Regulation of cellular activities	1.10E-15
7LCMGC028	ES790229	RNA-binding protein RZ-1	Protein synthesis	2.90E-25
7LCMGC029	ES790230	Glucose-6-phosphate 1-dehydrogenase, cytoplasmic isoform	Carbohydrate metabolism	3.10E-64
7LCMGC030	ES790231	40S ribosomal protein S8	Cellular component, protein synthesis	7.0E-49
7LCMGC031	ES790232	cDNA sequence {*L. esculentum*}	Unknown function	3.80E-08
7LCMGC032	ES790233	40S ribosomal protein S8	Cellular component, protein synthesis	1.2E-22
7LCMGC033	ES790234	Zinc finger A20 and AN1 domains-containing protein {*A. thaliana*}	Transcription	8.3E-96
7LCMGC034	ES790235	DNA-binding protein	Transcription	1.5E-37
7LCMGC035	ES790236	DNA-binding protein, MYB-CC type transfactor {*A. thaliana*}	Transcription	1.40E-44
7LCMGC036	ES790237	MTD1 {*Medicago truncatula*}	Unknown function	4.40E-38
7LCMGC037	ES790238	Glyceraldehyde-3-phosphate dehydrogenase, A subunit (GAPDH)	Metabolism, energy	4.30E-28
7LCMGC038	ES790239	Ribosomal protein L27	Cellular component, protein synthesis	2.10E-27
7LCMGC039	ES790240	U2AF (U2 snRNP auxiliary factor) small subunit	Transcription	6.00E-45
7LCMGC040	ES790241	Unknown protein {*A. thaliana*}	Unclassified proteins	5.90E-42
7LCMGC041	ES790242	Putative serine/arginine (SR) protein kinase protein	Signal transduction	4.6E-43
7LCMGC042	ES790243	Fibre protein Fb11	Unknown function	4.50E-54
7LCMGC043	ES790244	DNA-directed RNA polymerase II polypeptide K	Protein synthesis	3.10E-60
7LCMGC044	ES790245	Ribonucleoprotein complex subunit 2-like protein (Nhp2-like protein)	Transcription	1.20E-35
7LCMGC045	ES790246	Cytochrome *c* oxidase polypeptide Vc-2	Metabolism, electron transport	6.90E-52
7LCMGC046	ES790247	RAD23-like protein	DNA repair and protein modification	3.10E-64
7LCMGC047	ES790248	cDNA sequence {*L. esculentum*}	Unknown function	5.50E-49
7LCMGC048	ES790249	cDNA sequence {*Solanum tuberosum*}	Unknown function	1.00E-26
7LCMGC049	ES790250	Cytosolic ascorbate peroxidase	Metabolism, electron transport	2.90E-133
7LCMGC050	ES790251	Putative ethylene-responsive (ER6) protein (*A. thaliana*}	Regulation of cellular processes	2.2E-39
7LCMGC051	ES790252	Glycoprotein-like protein	Protein synthesis	1.00E-51
7LCMGC052	ES790253	Putative thioredoxin reductase {*Oryza sativa* cv. japonica}	Metabolism, electron transport	5.9E-29
7LCMGC053	ES790254	Glyoxalase I {*O. sativa* cv. japonica}	Carbohydrate metabolism	2.2E-15
7LCMGC054	ES790255	cDNA sequence {*S. tuberosum*}	Unknown function	2E-104

Table 3 Changes in expression of 25 selected genes between laser microdissected control cells and giant cells 4 and 7 days post-infection (dpi) revealed by real-time quantitative reverse transcriptase-polymerase chain reaction (RT-PCR).

Clone	Gene	Fold increase over uninfected tomato roots		Relative gene* expression pattern from before infection to 7 dpi
		4 dpi	7 dpi	
ZW0103001	Cysteine synthase	34.53 ± 0.31	68.59 ± 0.23	C ▲ 4 ▲ 7
ZW30050020	60S ribosomal protein L37A	28.84 ± 0.03	233.94 ± 0.08	C ▲ 4 ▲ 7
4LCMGC0080	Pathogenesis-related TSI-1 protein	28.05 ± 1.53	107.62 ± 0.59	C ▲ 4 ▲ 7
ZW0103003	SAMDC	24.25 ± 0.33	55.71 ± 0.26	C ▲ 4 ▲ 7
4LCMGC0032	Cytosolic Cu,Zn superoxide dismutase	17.87 ± 0.64	41.64 ± 0.41	C ▲ 4 ▲ 7
4LCMGC036	ELI3 protein	12.29 ± 0.14	25.99 ± 0.57	C ▲ 4 ▲ 7
ZW3107005	Cytochrome *c* reductase subunit	6.32 ± 0.34	19.97 ± 0.46	C ▲ 4 ▲ 7
4LCMGC039	LescPth2, serine/threonine protein kinase	4.47 ± 0.18	7.41 ± 0.61	C ▲ 4 ▲ 7
4LCMGC061	Zinc finger transcription factor-like protein	4.17 ± 0.27	9.71 ± 0.56	C ▲ 4 ▲ 7
4LCMGC002	Hydroxymethylglutaryl coenzyme A synthase	3.78 ± 0.31	5.24 ± 0.84	C ▲ 4 ▲7
ZW3107003	Cytochrome *c* oxidase subunit VIIa	1.83 ± 0.31	3.50 ± 0.43	C ▲ 4 ▲ 7
4LCMGC052	Calmodulin-binding protein	1.55 ± 0.09	2.80 ± 0.53	C ▲ 4 ▲ 7
4LCMGC003	Pyruvate dehydrogenase E1 α subunit	1.54 ± 0.32	3.20 ± 0.28	C ▲ 4 ▲ 7
4LCMGC0051	Pectinesterase U1 precursor	8.00 ± 0.36	7.31 ± 0.79	C ▲ 4 ≈ 7
ZW0903001	60S ribosomal protein L31	1.85 ± 0.36	1.85 ± 0.51	C ▲ 4 ≈ 7
4LCMGC075	Phi-1 protein	8.51 ± 0.26	6.73 ± 0.68	C ▲ 4 ▼ 7
ZW3107009	Unknown protein	1.04 ± 0.37	8.57 ± 0.21	C ≈ 4 ▲ 7
4LCMGC008	Clathrin-binding protein	0.67 ± 0.33	2.99 ± 0.27	C ≈ 4 ▲ 7
7LCMGC0036	MTD1	1.29 ± 0.31	2.03 ± 0.87	C ≈ 4 ▲ 7
4LCMGC001	Hypothetical protein	0.30 ± 0.47	1.82 ± 0.27	C ≈ 4 ▲ 7
4LCMGC0018	Transaldolase	0.78 ± 0.26	1.64 ± 0.29	C ≈ 4 ▲ 7
4LCMGC0012	Lipid transfer protein	0.64 ± 0.29	0.17 ± 0.30	C ≈ 4 ≈ 7
4LCMGC060	Phenylalanine ammonia-lyase	0.30 ± 0.08	0.15 ± 0.54	C ≈ 4 ≈ 7
4LCMGC0078	Microtubule-associated protein MAP65-1a	0.07 ± 0.46	0.16 ± 0.37	C ≈ 4 ≈ 7
4LCMGC0085	PIP-type aquaporin	0.01 ± 0.28	0.04 ± 0.04	C ≈ 4 ≈ 7

*Relative gene expression pattern was established using the fold change at each time point starting from expression levels in control cells to 4 and 7 dpi. The symbols ▼, ▲ and ≈ represent lower, higher or similar expression between time points.

cytosolic calcium ions, a process necessary for the control of several biological processes. A gene for each of the two types of calcium-binding protein was identified in the libraries: a calmodulin and a calmodulin-binding protein were identified from the 4-dpi library, whereas an annexin p34 was obtained from the 7-dpi library.

Temporal and spatial expression of giant cell transcripts

Real-time quantitative RT-PCR was used to study the expression levels of selected genes in giant cells. Twenty-five genes representing various metabolic pathways and cellular components/processes were chosen, including seven genes (ZW0103001–ZW0903001) previously known to be expressed in mature giant cells. Gene expression was quantified at two time points (4 and 7 dpi) using the comparative CT method (ΔΔCT) and the cytosolic glyceraldehyde 3-phosphate dehydrogenase (GAPDH) gene as an endogenous control. CT values were the means of three replicates. The relative gene expression at each time point was calculated with reference to expression in control cells obtained by LM, and a fold difference of 1.5 was considered as significantly up- or down-regulated (Table 3).

The expression patterns of these selected genes formed five different groups. Thirteen genes in group 1 showed continuously up-regulated expression from 4 to 7 dpi. This group also includes the highest expressed genes: a cysteine synthase with a 34.5-fold up-regulation at 4 dpi, and a 60S ribosomal protein L37A with a 234-fold increase at 7 dpi. Two genes in group 2, pectinesterase U1 precursor and 60S ribosomal protein L31, were up-regulated at 4 dpi and the expression remained the same at 7 dpi. Expression of the *Phi-1* gene in group 3 was highly up-regulated in giant cells at 4 dpi, and then decreased at 7 dpi. Five genes in group 4 showed no significant changes in expression at 4 dpi compared with control cells, but were up-regulated by 7 dpi. The expression of four genes in group 5 was not affected during the induction and development of giant cells, and the levels were the same as those in control cells at 4 and 7 dpi.

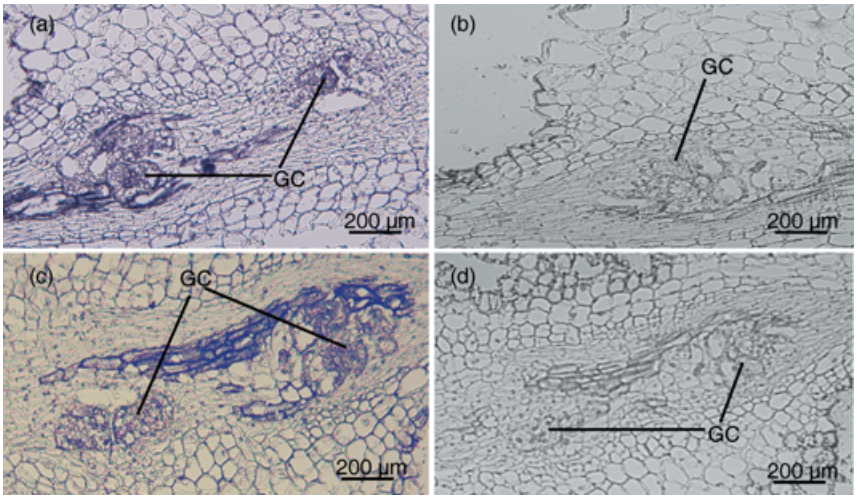

Fig. 2 *In situ* hybridization of *Meloidogyne javanica*-infected tomato root tissues at 4 days post-infection (dpi) with probes generated from a Phi-1 protein gene (A, B) and a pectinesterase-like protein gene (C, D). Strong signals are present in giant cells when hybridized with antisense probes (A, C) compared with sense probes (B, D). GC, giant cells.

The localization of expression of two genes, *Phi-1* and the pectinesterase U1 precursor, was studied further by *in situ* hybridization in gall tissues at 4 dpi. Individual EST clones of these genes identified in the libraries were used to synthesize sense and antisense digoxigenin-labelled probes employing T7 and SP6 RNA polymerase. Using the polymer polyvinyl alcohol, known to enhance formazan formation in alkaline phosphatase reactions, a strong hybridization signal was observed in tissues hybridized with antisense probes, with little background on tissues hybridized with sense probes (Fig. 2). Although most cells exhibited hybridization with the antisense probes, the signal was much stronger in developing giant cells than in the surrounding cells, indicating that these transcripts were preferentially expressed in the cytoplasm of giant cells.

DISCUSSION

The technique of LM has been applied to isolate specific cells and tissues for gene and protein profiling studies. We first demonstrated the isolation by LM of specific cytoplasmic contents of early developing giant cells induced by *M. javanica* (Ramsay *et al.*, 2004). Using the same technique, giant cell contents at 4 and 7 dpi have been isolated, and mRNA amplified from the captured cells was used to construct giant cell-specific cDNA libraries. More than 5000 clones were screened from both libraries by PCR and restriction digestion before sequencing. A total of 141 individual transcripts (87 and 54 from 4- and 7-dpi libraries, respectively) have been identified, which can be expected to play a role in the cellular processes important for giant cell formation, i.e. in metabolism, cell response to stress, protein synthesis, cell division and morphogenesis, transport, signal transduction, protein modification and fate, and regulation of cellular processes.

The isolation of giant cell contents by LM from sections of unstained gall tissue younger than 4 dpi is technically very demanding, because it is difficult to differentiate giant cell initials from surrounding cells (Ramsay *et al.*, 2004). Generally, by 6 dpi, giant cells are clearly multinucleate with enlarged nuclei and nucleoli, cell expansion is obvious and there are well-developed wall ingrowths (Jones, 1981; Jones and Payne, 1978). The induction and expansion phases of giant cells may be completed by 7–10 dpi, but changes in metabolism can occur up to maturity at 25–30 dpi (Ehsanpour and Jones, 1996). By dividing the analysis of the infection into two time points at 4 and 7 dpi, the aim was to study the processes involved in the induction and early-stage development of giant cells.

An appropriate endogenous control is important for the accuracy of quantitative RT-PCR analysis. The choice of GAPDH as a reference gene for the comparison of gene expression between nematode feeding cells and control tissues has been well discussed (Fuller *et al.*, 2007). We also confirmed the stability of expression of the GAPDH gene in giant cells. When the same amount of initial laser microdissected RNA was subjected to RT-PCR, there was no obvious difference in CT values of GAPDH between giant cells and control cells (data not shown). As shown in Table 3, most of the genes studied showed significant changes in expression between the two time points, and from control cells. The highest increase in expression was from a 60S ribosomal protein L37A gene, which was 29-fold at 4 dpi and 234-fold at 7 dpi, and a pathogenesis-related TSI-1 protein gene (28- and 108-fold, respectively). This 60S ribosomal protein L37A gene was also up-regulated in mature giant cells (Wang *et al.*, 2003). Another 60S ribosomal protein gene L31 showed increased expression at 4 dpi, and a similar level at 7 dpi. The up-regulation of other ribosomal protein genes induced in feeding cells has been reported previously (Vaghchhipawala *et al.*, 2001; Wang *et al.*,

2003), and this is consistent with a high level of protein synthesis in nematode feeding cells. Interestingly, there are two 60S ribosomal protein genes, L9 and L11, whose expression was suppressed in syncytia at 3 dpi according to an LM-associated microarray study (Klink *et al.*, 2007). How the reported suppression of these genes relates to increased ribosomes and protein synthesis in syncytia is not clear. The proliferation of ribosomes in giant cells clearly depends on the increased expression of ribosomal protein genes. However, in syncytia initials, there may be a contribution of ribosomes from neighbouring cells incorporated into syncytia that might account for the increased number of ribosomes.

Except for the *Phi-1* gene, all genes studied by real-time quantitative RT-PCR showed up-regulated or unchanged expression at 7 dpi compared with that at 4 dpi. In contrast, the *Phi-1* gene expression decreased at 7 dpi. *Phi-1* is a cell cycle-related gene which is also activated in phosphate-starved tobacco cell cultures when re-entry of the cell cycle is induced by the addition of phosphate (Farrar *et al.*, 2003; Sano *et al.*, 1999). The transcript level of the *Phi-1* gene in cultured cells then decreases with the start of DNA synthesis (Sano *et al.*, 1999). Cell cycle re-entry is a typical step of induction of giant cells at the early infection stage, and a number of cycle-related genes have been found to be up-regulated in giant cells (de Almeida Engler *et al.*, 1999; Goverse *et al.*, 2000, Ramsay *et al.*, 2004). It is possible that the induced activation of *Phi-1* gene expression occurs before 4 dpi, as giant cell initials re-enter the cell cycle, and subsequently expression decreases at 7 dpi. *In situ* hybridization results also indicate that expression of the *Phi-1* gene is located in giant cells at 4 dpi.

Another gene studied by quantitative RT-PCR and *in situ* hybridization, the pectinesterase U1 precursor gene, is up-regulated in giant cells at 4 and 7 dpi compared with that in control cells. Two more pectinesterase genes were identified in the 4-dpi library, which may be involved in cell wall modification, such as increased extensibility (Gaffe *et al.*, 1994; Wen *et al.*, 1999), during giant cell formation. There are other pectinesterase family genes up-regulated in the syncytia of soybean at 2 dpi; however, the expression of these genes was depressed in syncytia after 5 dpi (Ithal *et al.*, 2007a). These results are consistent with the different modes of formation of giant cells and syncytia, in that cell wall digestion is a fundamental process in the development of syncytia.

A knowledge of gene expression in nematode feeding cells is very important for an understanding of how feeding cells form and function. Large-scale gene expression profiling of host cells in response to nematode infection has been carried out by microarray studies on root tissues infected with root-knot (Jammes *et al.*, 2005) and cyst (Ithal *et al.*, 2007b; Khan *et al.*, 2004; Puthoff *et al.*, 2003, 2007) nematodes, and in more specific studies of individual feeding cells, for example syncytia by LM combined with cDNA library construction (Klink *et al.*, 2005) and microarray analysis (Ithal *et al.*, 2007a; Klink *et al.*, 2007). LM-associated microarray studies of giant cells have been limited by host plant and the availability of microarray chips covering full genome transcripts, such as for tomato as used in this study. In addition, even when the same Affymetrix soybean GeneChip was used in LM-associated microarray studies, there were significant differences between independent experiments. For example, Ithal *et al.* (2007a) identified 1765 genes (1116 up-regulated and 649 down-regulated with a 1.5-fold change cut-off) from laser microdissected syncytia samples of soybean infected with *H. glycines* at 2 dpi. Using the same technique, only 351 genes, 79 up-regulated and 272 down-regulated with a 1.5-fold change cut-off, were identified from laser microdissected soybean syncytia samples also infected with *H. glycines* at 3 dpi (Klink *et al.*, 2007). Although there were differences in the pathosystems used in these studies, in that different soybean cultivars and different *H. glycines* lines were used, the variation in the microarray data may result from the different statistical analysis approaches employed. The reliability and reproducibility of microarray results rely on appropriate data analysis practices, standardized if possible (Shi *et al.*, 2008). Nevertheless, microarray studies should be carried out on laser microdissected giant cell samples with the availability of appropriate genome chips and careful interpretation of the data.

In summary, we have successfully produced giant cell-specific cDNA libraries using LM from early-stage giant cell contents in tomato, and generated information on a set of genes whose functions and expression suggest possible involvement in the induction and development of giant cells. The temporal and spatial expression of some of the genes contrasts with events in developing syncytia. The genes identified from this work, and that of others, provide an indication of candidate genes for further studies in plant–nematode interactions. In addition, an understanding of the events occurring in nematode feeding sites may be aided by further studies of the uncharacterized transcripts found in the giant cell-specific libraries. Such work will provide more information for the future development of strategies to confer host resistance to endoparasitic nematodes.

EXPERIMENTAL PROCEDURES

LM of giant cells

In vitro culture of tomato cv. Grosse-lisse and infection with *M. javanica* were carried out as described previously (Hutangura *et al.*, 1999). Developing galls from infected roots and uninfected controls were collected at 4 and 7 dpi, and processed through tissue fixation, paraffin embedding and sectioning, as described previously (Ramsay *et al.*, 2004) with modifications. Fixed tissue was dehydrated at 4 °C in a graded ethanol series [(v/v) 75%, 85%, 90%, 100% and 100%] for 15 min each time on a rotator. This

was followed by an ethanol : xylene series [(v/v) 3 : 1, 1 : 1, 1 : 3], and then 100% xylene for 1.5 h (3 × 30 min). Tissue sections were then deparaffinized, microdissected (Ramsay *et al.*, 2004) using a PALM Robot-Combi LM system (PALM, Bernried, Germany) and catapulted into a flat cap of a 0.5-mL Eppendorf tube containing 40 μL of diethylpyrocarbonate (DEPC)-treated water with 40 U of RNasin RNase inhibitor (Promega, Sydney, Australia). One hundred cells were collected from galls at 4 and 7 dpi, and also from cells close to the vasculature of uninfected control roots.

RNA extraction and linear amplification

Total RNA from laser microdissected cells was extracted with the PicoPure RNA isolation kit (Arcturus Bioscience, Mountain View, CA, USA) according to the manufacturer's instructions. RNA was eluted with 30 μL of elution buffer and later concentrated in a vacuum centrifuge to approximately 10 μL, and quantified with a NanoDrop ND-1000 UV–visible spectrophotometer (Biolab Limited, Scoresby, Victoria, Australia). The RNA was then amplified using the SuperScript RNA amplification system (Invitrogen Corporation, Carlsbad, CA, USA) according to the manufacturer's protocol. Typically, this involved first-strand cDNA synthesis from approximately 100 ng of total RNA with Superscript III reverse transcriptase and T7-Oligo(dT), followed by second-strand cDNA synthesis by DNA polymerase I and DNA ligase, purification of cDNA with a spin cartridge and *in vitro* transcription using T7 polymerase.

cDNA synthesis and cloning

cDNAs for the 4- and 7-dpi giant cell-specific libraries were synthesized using the SuperScript RNA amplification system with modifications. For each (replicate) cDNA construction, first-strand cDNA was synthesized from 500 ng of aRNA in separate reactions using random hexamers and Oligo-dT. Reactions containing random hexamers were incubated at 25 °C to ensure that the primers annealed well before incubation at 46 °C for 2 h. This was immediately followed by double-stranded cDNA construction at 16 °C for 4 h. The dscDNA was first extracted with tris(hydroxymethyl)aminomethane–ethylenediaminetetraacetic acid (Tris-EDTA)-buffered phenol–chloroform–isoamyl alcohol (25 : 24 : 1) and precipitated with 20 μg of Glycogen (Sigma, Castle Hill, New South Wales, Australia), 7.5 M ammonium acetate and 2.5 vol of ethanol. cDNA was then separately A-tailed with 100 μM of dATP and 5 U of *Taq* DNA polymerase (Invitrogen Corporation) at 70 °C for 2 h, and 15 U of terminal deoxynucleotidyl transferase (Invitrogen Corporation) at 37 °C for 2 h. A total of 500–550 ng of A-tailed dscDNA was ligated to pGEM-T Easy. The ligated DNA was used to transform JM109 competent cells (Promega), and the colonies were selected with isopropyl-β-D-thiogalactopyranoside (IPTG) and 5-bromo-4-chloro-3-indolyl-β-D-galactopyranoside (X-Gal).

Library screening and sequencing

Positively identified transformed colonies were further analysed by PCR using T7 and SP6 primers. The PCRs were made up to 20 μL with water containing 0.2 mM deoxynucleoside triphosphate (dNTP), 2 mM $MgCl_2$, 5 pmol of primers, 0.25 U of recombinant *Taq* DNA polymerase and 1 × *Taq* buffer (Invitrogen Corporation), and 5 μL of individual colonies were resuspended in 20 μL of water as template. Selected cDNA clones were sequenced with the universal T7 primer; ambiguous bases were clarified by a further sequencing of the opposite strand with SP6 primer using Big Dye Terminator v3.1 chemistry, and electrophoresed with an AB3730 capillary sequencer (Perkin Elmer Life Sciences, Melbourne, Australia).

Sequence analysis and transcripts in the library

Raw sequences of the transcripts were edited using FinchTV Version 1.4.0 (http://www.geospiza.com/finchtv). For each library, multiple alignment using SeqEd V1.0.3 (Applied Biosystems, Foster City, CA, USA) and clustering of all sequences using ClustalW2 (http://www.ebi.ac.uk/Tools/clustalw2/index.html) were carried out to detect and remove duplicate sequences. ClustalW2 was also used to compare transcripts from both libraries to identify common transcripts. Edited sequences were employed to search for homologous sequences using BLAST (Altschul *et al.*, 1990) made available by The Gene Index (TGI) Project (http://compbio.dfci.harvard.edu/tgi), with the tomato gene index database from the TGI Project as a primary database to identify tomato genes. The nucleotide and EST collection maintained by the NCBI was also used to search for transcripts with no homologues on the primary database. Sequences with significant matches had a cut-off expected value of 1E-5 for which the most homologous was presented. The functions or functional categories of the transcripts were inferred from descriptions or homologues deposited in the TGI project and NCBI, and were confirmed using UNIProt (http://beta.uniprot.org) and the *Kyoto Encyclopaedia of Genes and Genomes* (http://www.genome.jp/kegg).

Real-time quantitative RT-PCR

Real-time quantitative RT-PCR was carried out using a Corbett Rotor Gene RG-3000 (Corbett Research, Brisbane, Queensland, Australia). Specific primers for the target genes were designed with Primer 3 (v.0.4.0) (http://frodo.wi.mit.edu). aRNA used as template for quantitative PCR was reverse transcribed using the High-Capacity cDNA Reverse-Transcription Kit, according to the manufacturer's protocol (Applied Biosystems, CA, USA). Quantitative PCRs were performed in triplicate with Power SYBR Green PCR Master Mix, and contained 1 μL of template cDNA and 500 nM of each primer made up to a volume of 20 μL with

RNase-free sterile water. The PCR conditions used were as follows: a hold at 95 °C for 10 min, 45 cycles of denaturation at 95 °C for 10 s, and annealing and acquisition at 55 °C for 1 min, except for three genes where the annealing and acquisition of the data were performed at 50 °C for 1 min. Gene expression was quantified using the comparative CT method (ΔΔCT), as described by the *Real Time PCR Handbook*, with a tomato GAPDH gene as an endogenous control (http://www.uic.edu/depts/rrc/cgf/realtime/deltact.html).

In situ hybridization

Gall tissues were trimmed from infected tomato roots at 4 dpi and fixed immediately in formalin–acetic acid (50% ethanol; 10% formalin containing 37% formaldehyde; 5% acetic acid) at room temperature for 4 h, with vacuum infiltration at 400 mmHg once every hour, followed immediately by a change of the fixative. Fixed tissues were dehydrated in an ethanol series: 50% for 3×30 min, 75% for 1.5 h (both at room temperature) and 85% at 4 °C overnight. The tissues were transferred to a Leica TP 1020 (Leica Microsystems, North Ryde, New South Wales, Australia) automated tissue processing system for further dehydration in a series of 90% and 100% ethanol (1.5 h each time) and then chloroform, before embedding in molten wax. Paraffin-embedded tissues were sectioned into ribbons, 10 μm thick, floated in DEPC-treated water at 42 °C and mounted onto silane-coated slides. PCR products with T7 and SP6 promoter sequences appended to the termini were used to produce labelled RNA probes which were synthesized using the DIG RNA Labelling Kit (Roche Applied Science, Castle Hill, New South Wales, Australia) according to the manufacturer's instructions. *In situ* hybridizations were performed essentially as described by DeBlock and Debrouwer (2002) using polyvinyl alcohol (40–88 kDa) for enhanced visualization.

ACKNOWLEDGEMENTS

We thank Dr Kathryn Heel-Miller (Lotteries Laser Microdissection Facility, University of Western Australia, Perth, Australia) for assistance with LM. We also thank Mr Gordon Thomson (Murdoch University, Perth, Australia) for advice in tissue processing. This research was supported an Australian Research Council Discovery Grant (A00105534).

REFERENCES

Altschul, S.F., Gish, W., Miller, W., Myers, E.W. and Lipman, D.J. (1990) Basic local alignment search tool. *J. Mol. Biol.* **215**, 403–410.

Bird, D.M. and Wilson, M.A. (1994) DNA-sequence and expression analysis of root-knot nematode-elicited giant-cell transcripts. *Mol. Plant–Microbe Interact.* **7**, 419–424.

Davis, E.L., Hussey, R.S., Baum, T.J., Bakker, J., Schots, A., Rosso, M. and Abad, P. (2000) Nematode parasitism genes. *Annu. Rev. Phytopathol.* **38**, 365–396.

Day, R.C., Grossniklaus, U. and Macknight, R.C. (2005) Be more specific! Laser-assisted microdissection of plant cells. *Trends Plant Sci.* **10**, 397–406.

de Almeida Engler, J., De Vleesschauwer, V., Burssens, S., Celenza, J.L., Inzè, D., Von Montagu, M., Engler, G. and Gheysen, G. (1999) Molecular markers and cell cycle inhibitors show the importance of cell cycle progression in nematode-induced galls and syncytia. *Plant Cell*, **11**, 793–807.

de Almeida Engler, J., van Poucke, K., Karimi, M., De Groodt, R., Gheysen, G., Engler, G. and Gheysen, G. (2004) Dynamic cytoskeleton rearrangements in giant cells and syncytia of nematode-infected roots. *Plant J.* **38**, 12–26.

DeBlock, M. and Debrouwer, D. (2002) RNA–RNA in situ hybridization using DIG-labeled probes: the effect of high molecular weight polyvinyl alcohol on the alkaline phosphatase indoxyl-nitroblue tetrazolium reaction. In: *Procedures for In Situ Hybridization to Chromosomes, Cells, and Tissue Sections* (Doris Eisel, Stefanie Grünewald-Janho, Bettina Kruchen, eds). Penzberg, Germany: Roche Applied Science, pp. 172–176.

Ehsanpour, A.A. and Jones, M.G.K. (1996) Glucuronidase expression in transgenic tobacco roots with a *Parasponia* promoter on infection with *Meloidogyne javanica*. *J. Nematol.* **28**, 407–413.

Escobar, C., Barcala, M., Portillo, M., Almoguera, C., Jordano, J. and Fenoll, C. (2003) Induction of the Hahsp*17.7G4* promoter by root-knot nematodes: involvement of heat-shock elements in promoter activity in giant cells. *Mol. Plant–Microbe Interact.* **16**, 1062–1068.

Farrar, K., Evans, I.M., Topping, J.F., Souter, M.A., Nielsen, J.E. and Lindsey, K. (2003) EXORDIUM—a gene expressed in proliferating cells and with a role in meristem function, identified by promoter trapping in Arabidopsis. *Plant J.* **33**, 61–73.

Favery, B., Lecomte, P., Gil, N., Bechtold, N., Bouchez, D., Dalmasso, A. and Abad, P. (1998) RPE, a plant gene involved in early developmental steps of nematode feeding cells. *EMBO J.* **17**, 6799–6811.

Favery, B., Chelysheva, L.A., Lebris, M., Jammes, F., Marmagne, A., de Almeida-Engler, J., Lecomte, P., Vaury, C., Arkowitz, R.A. and Abad, P. (2004) Arabidopsis formin AtFH6 is a plasma membrane associated protein upregulated in giant cells induced by parasitic nematodes. *Plant Cell*, **16**, 2529–2540.

Fuller, V.l., Lilley, C.J., Atkinson, H.J. and Urwin, P.E. (2007) Differential gene expression in Arabidopsis following infection by plant-parasitic nematodes *Meloidogyne incognita* and *Heterodera schachtii*. *Mol. Plant Pathol.* **8**, 595–609.

Gaffe, J., Tieman, D.M. and Handa, A.K. (1994) Pectin methylesterase isoforms in tomato (*Lycopersicon esculentum*) tissues. *Plant Physiol.* **105**, 199–203.

Gheysen, G. and Fenoll, C. (2002) Gene expression in nematode feeding sites. *Annu. Rev. Phytopathol.* **40**, 191–219.

Goddijn, O.J.M., Lindsey, K., van der Lee, F.M., Klap, J.C. and Sijmons, P.C. (1993) Differential gene expression in nematode-induced feeding structures of transgenic plants harbouring promoter-*gusA* fusion constructs. *Plant J.* **4**, 863–873.

Goverse, A., de Almeida Engler, J., Verhees, J., van der Krol, S., Helder, J. and Gheysen, G. (2000) Cell cycle activation by plant parasitic nematodes. *Plant Mol. Biol.* **43**, 747–761.

Hutangura, P., Mathesius, U., Jones, M.G.K. and Rolfe, B.G. (1999) Auxin induction is a trigger for root gall formation caused by root-knot

nematodes in white clover and is associated with the activation of the flavonoid pathway. *Aust. J. Plant Pathol.* **26**, 221–231.

Ithal, N., Recknor, J., Nettleton, D., Hearne, L., Maier, T., Baum, T.J. and Mitchum, M.G. (2007a) Parallel genome-wide expression profiling of host and pathogen during soybean cyst nematode infection of soybean. *Mol. Plant–Microbe Interact.* **3**, 293–305.

Ithal, N., Recknor, J., Nettleton, D., Maier, T., Baum, T.J. and Mitchum, M.G. (2007b) Developmental transcript profiling of cyst nematode feeding cells in soybean roots. *Mol. Plant–Microbe Interact.* **20**, 510–525.

Jammes, F., Lecomte, P., de Almeida Engler, J., Bitton, F., Martin-Magniette, M.L., Renou, J.P., Abad, P. and Favery, B. (2005) Genome-wide expression profiling of the host response to root-knot nematode infection in Arabidopsis. *Plant J.* **44**, 447–458.

Jones, M.G.K. (1981) Host cell responses to endoparasitic nematode attack; structure and function of giant cells and syncytia. *Annu. Appl. Biol.* **97**, 353–372.

Jones, M.G.K. and Dropkin, V.H. (1976) Scanning electron microscopy of nematode-induced giant transfer cells. *Cytobios*, **15**, 149–161.

Jones, M.G.K. and Payne, H.L. (1978) Early stages of nematode-induced giant-cell formation of roots of *Impatiens balsamina*. *J. Nematol.* **10**, 70–83.

Juergensen, K., Scholz-Starke, J., Sauer, N., Hess, P., van Bel, A.J.E. and Grundler, F.M.W. (2003) The companion cell-specific Arabidopsis disaccharide carrier AtSUC2 is expressed in nematode-induced syncytia. *Plant Physiol.* **131**, 61–69.

Khan, R., Alkharouf, N., Beard, H., MacDonald, M., Chouikha, I., Meyer, S., Grefenstette, J., Knap, H. and Matthews, B. (2004) Microarray analysis of gene expression in soybean roots susceptible to the soybean cyst nematode two days post invasion. *J. Nematol.* **36**, 241–248.

Klink, V.P., Alkharouf, N., MacDonald, M. and Matthews, B. (2005) Laser capture microdissection (LCM) and expression analyses of *Glycine max* (soybean) syncytium containing root regions formed by the plant pathogen *Heterodera glycines* (soybean cyst nematode). *Plant Mol. Biol.* **59**, 965–979.

Klink, V.P., Overall, C.C., Alkharouf, N.W., MacDonald, M.H. and Matthews, B.F. (2007) Laser capture microdissection (LCM) and comparative microarray expression analysis of syncytia cells isolated from incompatible and compatible soybean (*Glycine max*) roots infected by the soybean cyst nematode (*Heterodera glycines*). *Planta*, **226**, 1389–1409.

Lohar, D.P., Schaff, J.E., Laskey, J.G., Kieber, J.J., Bilyeu, K.D. and Bird, D.M. (2004) Cytokinins play opposite roles in lateral root formation, and nematode and rhizobial symbioses. *Plant J.* **38**, 203–214.

Puthoff, D.P., Nettleton, D., Rodermel, S.R. and Baum, T.J. (2003) Arabidopsis gene expression changes during cyst nematode parasitism revealed by statistical analyses of microarray expression profiles. *Plant J.* **33**, 911–921.

Puthoff, D.P., Ehrenfried, M.L., Vinyard, B.T. and Tucker, M.L. (2007) GeneChip profiling of transcriptional responses to soybean cyst nematode, *Heterodera glycines*, colonization of soybean roots. *J. Exp. Bot.* **58**, 3407–3418.

Ramsay, K., Wang, Z. and Jones, M.G.K. (2004) Using laser capture microdissection to study gene expression in early stages of giant cells induced by root-knot nematodes. *Mol. Plant Pathol.* **5**, 587–592.

Ramsay, K., Jones, M.G.K. and Wang, Z. (2006) Laser capture microdissection: a novel approach to microanalysis of plant–microbe interactions. *Mol. Plant Pathol.* **7**, 429–435.

Sano, T., Kuraya, Y., Amino, S. and Nagata, T. (1999) Phosphate as a limiting factor for the cell division of tobacco BY-2 cells. *Plant Cell Physiol.* **40**, 1–8.

Shi, L., Perkin, R.G., Fang, H. and Tong, W. (2008) Reproducible and reliable microarray results through quality control: good laboratory proficiency and appropriate data analysis practices are essential. *Curr. Opin. Biotechnol.* **19**, 10–18.

Vaghchhipawala, Z., Bassüner, R., Clayton, K., Lewers, K., Shoemaker, R. and Mackenzie, S. (2001) Modulations in gene expression and mapping of genes associated with cyst nematode infection of soybean. *Mol. Plant–Microbe Interact.* **14**, 42–54.

Wang, Z., Potter, R.H. and Jones, M.G.K. (2003) Differential display analysis of gene expression in the cytoplasm of giant cells induced in tomato roots by *Meloidogyne javanica*. *Mol. Plant Pathol.* **4**, 361–371.

Wen, F., Zhu, Y. and Hawes, M.C. (1999) Effect of pectin methylesterase gene expression on pea root development. *Plant Cell*, **11**, 1129–1140.